

The Potential Flow Signature of a Turbulent Spot

C.W. VAN ATTA

Professor of Engineering Sciences and Oceanography, University of California, San Diego, USA

M. SOKOLOV

Tel Aviv University, Israel

R.A. ANTONIA

Professor of Mechanical Engineering, The University of Newcastle

and

A.J. CHAMBERS

Senior Lecturer in Mechanical Engineering, The University of Newcastle

SUMMARY The organized laminar flow disturbance produced in the free stream above a spark-generated turbulent spot in a laminar boundary layer has been measured and the results compared with a two-dimensional potential flow theory based on integral properties of the structure of the turbulent region within the spot. The regions of largest longitudinal potential flow disturbance occur at 1.5 spot heights above the surface and are anticorrelated in time and location with those regions of largest ensemble mean disturbance within the turbulent spot. The largest positive and negative potential perturbations are located above the forward and rear primary foci identified as points of accumulation for particle paths by Cantwell et al. (1978) and as extremal points for ensemble mean temperature and velocity perturbations by Van Atta and Helland (1980) and Zilberman et al. (1977). The boundary layer displacement thickness δ^* measured through the spot on its centerline as a function of time was used to construct a two-dimensional model for the potential flow above the spot. Using the conical similarity assumption reduces the problem to solving for the linearized quasi-steady potential flow field around a moving, growing, bump on the wall, the shape of the bump being given by the δ^* distribution. The numerical results obtained with this model exhibit all the main features of the potential flow field observed experimentally. The shapes and amplitudes of the calculated waveform at all y locations are in good general agreement with the experimental data. Near the wall the model predicts too short an arrival time for the first minimum, but the arrival times of successive maxima and minima are well predicted. The results suggest that a potential flow analysis accounting for the three-dimensional structure of the spot could improve the agreement.

1 EXPERIMENTAL APPARATUS AND MEASUREMENTS

The measurements were made at a nominal free stream velocity U_∞ of 11 m/s in the closed circuit wind tunnel of the Department of Applied Mechanics and Engineering Sciences at the University of California, San Diego. The tunnel has a 76 cm \times 76 cm \times 10 m working section. The plexiglass ceiling of this section was mounted on jacks to allow adjustment of the pressure gradient. The flat plate on which the laminar boundary layer developed was also mounted on jacks and located in a nearly horizontal position at a height of approximately 28 cm above the working section floor. The longitudinal turbulence level is less than 0.05% at a speed of 10 m/s at the exit plane of the 13:1 contraction. The polished aluminum flat plate was 1.27 cm thick and 2.44 m in length, and spanned the complete width of the working section. The upstream part of the plate was machined to include a wedge angle of 30°. The leading edge of the plate was located at a distance of 24 cm from the entrance to the working section. The present experimental set up and conditions are similar to those of Van Atta and Helland (1980) and Antonia et al. (1980), for which the plate was also heated.

Turbulent spots were generated by a capacitive discharge between stainless steel sewing needles (diameter \approx 0.1 mm, spanwise separation \approx 2 mm) protruding a distance of 1 mm into the boundary layer at a distance of 29 cm from the plate leading edge and located on the tunnel center line ($z = 0$).

The needles did not produce transition in the absence of the spark. The frequency of the square wave used to trigger the spark discharge unit was 2 Hz. As firings of the spark occurred at both positive and negative crossings of the square wave, the duration between discharges was 250 ms.

The measurements presented here were obtained at a distance $x_s = 106$ cm from the spark, on the centerline ($z = 0$). The streamwise pressure gradient, measured with pressure tappings along the ceiling of the working section, was found to be small and favorable. It was approximately constant, with an average of

$$\frac{1}{\frac{1}{2}\rho U_\infty^2} \frac{dp}{dx} \approx -1.4 \times 10^{-3} \text{ cm}^{-1}$$

for a streamwise distance over which measurements were taken.

The instantaneous longitudinal velocity $u(x, y, t)$ was measured with a 5 μ m diameter Wollaston wire (Pt-10% Rh, length 1 mm) operated by a DISA 55M10 constant temperature anemometer at an overheat of 0.8. The hot wire was calibrated in the free stream at the x_s location at which the experiment was conducted. The free stream velocity was measured with a Pitot static tube connected to an MKS Baratron pressure transducer.

Mean velocity profiles measured with the spot generator switched off have been presented by Antonia

et al. and are in good agreement with the Blasius profile. At $x_s = 106$ cm, the boundary layer thickness δ ($U = 0.995 U_\infty$) is 0.7 cm while the displacement thickness δ^* and momentum thickness θ are 0.218 cm and 0.084 cm, respectively. The longitudinal component of the unsteady flow above the growing spot was measured as a function of time at fifteen vertical (y) locations above the plate extending to roughly fifteen spot heights or thirty laminar boundary layer thicknesses. Ensemble averaging over several hundred spots was used to improve the signal to noise ratio.

Voltages from the hot wire were recorded after being passed through buck and gain units on a 4-track FM tape recorder (Hewlett-Packard 3960A). The square wave spark generator signal was also recorded. The signals were later played back at the same tape speed as recording (9.52 cm/s) and digitized (12 bit, including sign, A-D converter) at a sampling frequency of 3000 Hz into a digital computer. Typically, 720 samples (corresponding to a real time of 230 ms) were stored on magnetic tape for each spot realization, the sampling being triggered by the square wave. As illustrated in Fig. 4, for large values of y , the potential flow spot signature is a single cycle of roughly sinusoidal form, while just above the spot a convoluted waveform with two local minima is observed during passage of the spot.

A contour plot of the ensemble averaged disturbance velocity relative to laminar values is shown in Figure 1, together with corresponding contours within the turbulent spot from Antonia et al. (1980). The maximum positive and negative potential perturbations lie almost directly above corresponding negative and positive maxima within the turbulent spot, at a height of about 1.5 spot heights as defined by the one percent disturbance velocity in the turbulent spot. The largest perturbations are located above the two primary foci as identified by CCD, while the forward weaker negative maximum is associated with a weaker, non-focal region of velocity excess under the forward tip of the spot, which cannot be seen in the compressed scale used in the figure. The strength of the potential disturbance is still 0.1% of U_∞ at ten spot heights, and

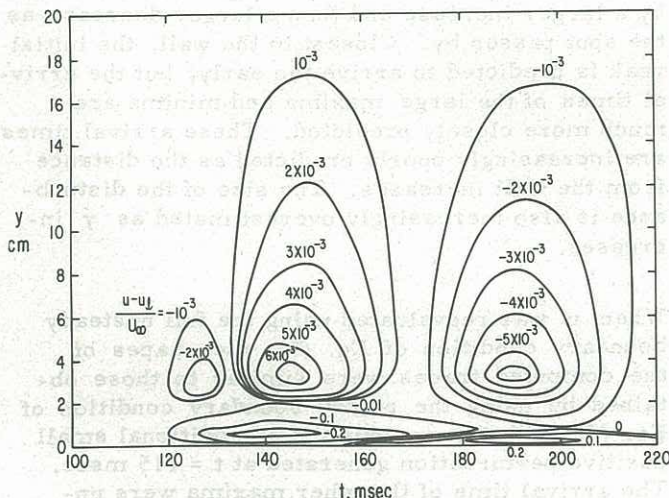


Figure 1 The longitudinal velocity disturbance relative to laminar values. Here and in succeeding figures $t=0$ at the firing of the spark.

can be detected out to fifteen spot heights, or thirty laminar boundary layer thicknesses.

2 THEORY AND COMPARISON WITH EXPERIMENT

At any given time, t , we assume that the disturbance produced in the outer potential flow is that caused by a two-dimensional solid body having a shape given by the instantaneous distribution of displacement thickness $\delta^*(x, t)$ as calculated from the ensemble mean velocity profiles measured on the centerline of the turbulent spot. We choose a dimensionless similarity variable,

$$\xi = \frac{(x - x_0)}{U_\infty (t - t_0)},$$

as introduced for the turbulent spot by Cantwell, Coles and Dimotakis (1978), where x_0 and t_0 , specify the apparent origin of the spot. The dimensionless displacement thickness is then given by

$$\frac{\delta^*}{U_\infty (t - t_0)} = f(\xi) \quad (1)$$

To solve the quasi-steady potential flow problem requires δ^* as a function of x for fixed t . Because of the similarity assumption, the function $f(\xi)$ can be determined from the δ^* data obtained at fixed x for variable t . Since the spot is very thin in the y direction compared with its length in x , the steady linearized boundary condition for the vertical (y) velocity component $v(x, y, t)$ is

$$\frac{v}{U_\infty} = \frac{d\delta^*}{dx} \quad \text{at } y = 0. \quad (2)$$

Then, from potential flow theory (e.g., Cole (1946)) the velocity components u and v , in the x and y directions, respectively, are given by

$$\frac{u(x, y, t)}{U_\infty} = -\frac{1}{\pi} \int_{-\infty}^{\infty} \frac{\frac{d\delta^*}{dx}(s, t)(s-x)ds}{(s-x)^2 + y^2} \quad (3)$$

$$\frac{v(x, y, t)}{U_\infty} = \frac{y}{\pi} \int_{-\infty}^{\infty} \frac{\frac{d\delta^*}{dx}(s, t)ds}{(s-x)^2 + y^2} \quad (4)$$

Noting, from (1), that $d\delta^*/dx = f'(\xi)$, where a prime denotes differentiation with respect to ξ , a change of the variable of integration yields

$$\frac{u(x, y, t)}{U_\infty} = -\frac{1}{\pi} \int_{-\infty}^{\infty} \frac{f'(\xi)(x - \xi) d\xi}{(x - \xi)^2 + \eta^2} \quad (5)$$

$$\frac{v(x, y, t)}{U_\infty} = \frac{\eta}{\pi} \int_{-\infty}^{\infty} \frac{f'(\xi) d\xi}{(x - \xi)^2 + \eta^2} \quad (6)$$

$$\eta = y/U_\infty(t-t_0).$$

The complete linearized unsteady boundary condition for a solid body of time varying shape is

$$\frac{v(x, 0, t)}{U_\infty} = \frac{1}{U_\infty} \frac{\partial \delta^*}{\partial t} + \frac{\partial \delta^*}{\partial x} = f(\xi) + (1-\xi)f' \text{ at } y=0 \quad (7)$$

In this case the expressions for u and v are similar, with f' being replaced by $f + (1-\xi)f'$ in Eqs. (5) and (6). The values of δ^* calculated as a function of time from measurements at $x = 135$ cm (Antonia et al., 1980) are shown in Figure 2. The functions $f(\xi)$ and $f'(\xi)$ calculated

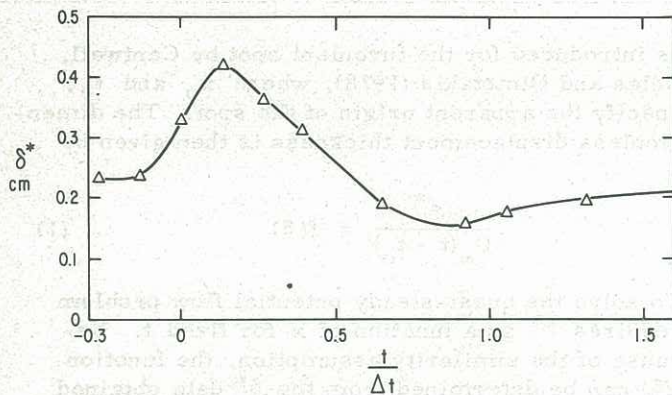


Figure 2 Displacement thickness δ^* at $x = 135$ cm as a function of time, computed from instantaneous velocity profiles within the turbulent spot.

from the curve fit to the δ^* data in Figure 2 are shown in Figure 3. Using this data, the integrals in Eqs. (5) and (6) were evaluated numerically for $x = 135$ cm and various values of y and t . A comparison of the numerical results with the individual ensemble averaged time traces at various y locations is shown in Figure 4. The general shape and magnitude of the potential disturbance velocity vs. time traces is correctly predicted. Near the wall, an initial decrease in velocity is followed

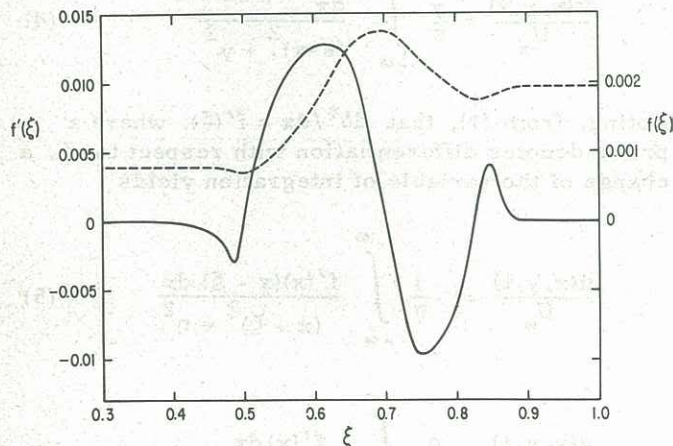


Figure 3 The functions f and f' computed from the measured δ^* .

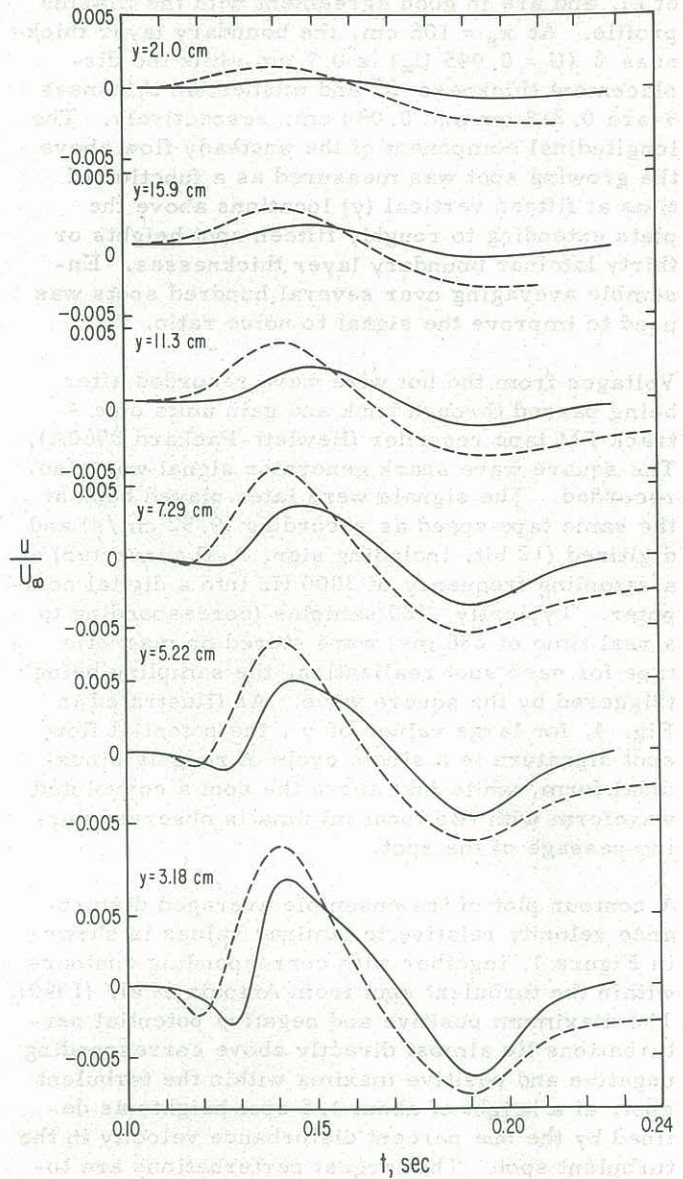


Figure 4 The longitudinal component of velocity $u(x, y, t)$ of the spot signature at $x = 135$ cm as a function of time at various heights y above the plate. —, measured. ---, two-dimensional potential theory.

by a larger increase and then a larger decrease, as the spot passes by. Closest to the wall, the initial peak is predicted to arrive too early, but the arrival times of the large maxima and minima are much more closely predicted. These arrival times are increasingly poorly predicted as the distance from the wall increases. The size of the disturbance is also increasingly overestimated as y increases.

When u was reevaluated using the full unsteady boundary condition of Eq. (7), the shapes of the computed traces were similar to those obtained by using the steady boundary condition of Eq. (2), with the exception of an additional small positive perturbation generated at $t = 115$ msec. The arrival time of the other maxima were unchanged, but their amplitudes were considerably reduced. It was concluded that the full unsteady boundary condition for a solid body is not as

appropriate as the quasi-steady one for representing the effect of the spot on the external flow.

It would be interesting to see if the computer signature of $u(x, y, t)$ produced by a three-dimensional calculation would agree better with the data. This calculation would require data for $\delta^*(x, t)$ from several lateral positions off the spot centerline.

3 CONCLUSIONS

The unsteady potential flow signatures generated by a turbulent spot can be fairly well represented by a two-dimensional similarity calculation for the flow over a moving bump on the wall, whose shape is given by the instantaneous displacement thickness distribution along the wall on the spot centerline. If the fully turbulent boundary layer can be represented as a flow containing a collection of turbulent spots then one might expect to see similar signatures in the potential flow outside the fully turbulent layer. The present results might be useful for devising a scheme for detecting the passage of spot-like flow structures within the turbulent layer using a probe in the free stream.

4 ACKNOWLEDGMENT

This work was supported by NSF Grant ENG78-25088 and the Australian Research Grants Committee.

5 REFERENCES

- ANTONIA, R.A., CHAMBERS, A.J., SOKOLOV, M. and VAN ATTA, C.W. (1980). Velocity and temperature characteristics of a turbulent spot in a laminar boundary layer (submitted to J. Fluid Mech.).
- CANTWELL, B., COLES, D. and DIMOTAKIS, P. (1978). Structure and entrainment in the plane of symmetry of a turbulent spot. J. Fluid Mech., Vol. 87, pp 641-672.
- COLE, J.D. (1946). On the transonic flow past thin airfoils. Aero. Engr. Thesis, California Institute of Technology Unpublished.
- VAN ATTA, C.W. and HELLAND, K.N. (1980). Exploratory temperature tagging measurements of turbulent spots in a heated laminar boundary layer. J. Fluid Mech. (in press). See also, Proc. IUTAM Symposium on Laminar-Turbulent Transition, University of Stuttgart, Sept. 1979, Springer-Verlag.
- WYGNANSKI, I., SOKOLOV, N. and FRIEDMAN, D. (1976). On the turbulent 'spot' in a boundary layer undergoing transition. J. Fluid Mech., Vol. 78, pp 785-819.
- ZILBERMAN, M., WYGNANSKI, I. and KAPLAN, R.E. (1977). Transitional boundary layer spot in a fully turbulent environment. Phys. Fluids, Vol. 20, pp S258-271.